Mechanism of Block of Single Protopores of the *Torpedo* Chloride Channel ClC-0 by 2-(*p*-Chlorophenoxy)butyric Acid (CPB)

Michael Pusch,[1] Alessio Accardi,[1] Antonella Liantonio,[2] Loretta Ferrera,[1] Annamaria De Luca,[2] Diana Conte Camerino,[2] and Franco Conti[1]

[1]Istituto di Cibernetica e Biofisica, Consiglio Nazionale delle Ricerche, I-6149 Genova, Italy
[2]Unità di Farmacologia, Dipartimento Farmacobiologico, Università di Bari, 70126, Bari, Italy

ABSTRACT We investigated in detail the mechanism of inhibition by the S(−) enantiomer of 2-(*p*-chlorophenoxy)butyric acid (CPB) of the *Torpedo* Cl^- channel, ClC-0. The substance has been previously shown to inhibit the homologous skeletal muscle channel, CLC-1. ClC-0 is a homodimer with probably two independently gated protopores that are conductive only if an additional common gate is open. As a simplification, we used a mutant of ClC-0 (C212S) that has the common gate "locked open" (Lin, Y.W., C.W. Lin, and T.Y. Chen. 1999. *J. Gen. Physiol.* 114:1–12). CPB inhibits C212S currents only when applied to the cytoplasmic side, and single-channel recordings at voltages (V) between −120 and −80 mV demonstrate that it acts independently on individual protopores by introducing a long-lived nonconductive state with no effect on the conductance and little effect on the lifetime of the open state. Steady-state macroscopic currents at −140 mV are half-inhibited by ~0.5 mM CPB, but the inhibition decreases with V and vanishes for V ≥ 40 mV. Relaxations of CPB inhibition after voltage steps are seen in the current responses as an additional exponential component that is much slower than the gating of drug-free protopores. For V ≤ −40 mV, where a significant inhibition is observable for the CPB concentrations used in this study (≤10 mM), the concentration dependence of its onset kinetics is consistent with CPB binding according to a bimolecular reaction. At all voltages, only the openings of drug-free protopores appear to contribute significantly to the current observed at any time. Lowering internal Cl^- hastens significantly the apparent "on" rate, suggesting that internal Cl^- antagonizes CPB binding to closed pores. Vice versa, lowering external Cl^- reduces the apparent rate of CPB dissociation from open pores. We studied also the point mutant K519E (in the context of the C212S mutant) that has altered conduction properties and slower single protopore gating kinetics. In experiments with CPB, the mutant exhibited drastically slowed recovery from CPB inhibition. In addition, in contrast to WT (i.e., C212S), the mutant K519E showed also a significant CPB inhibition at positive voltages (≥60 mV) with an IC_{50} of ~30–40 mM. Altogether, these findings support a model for the mechanism of CPB inhibition in which the drug competes with Cl^- for binding to a site of the pore where it blocks permeation. CPB binds preferentially to closed channels, and thereby also strongly alters the gating of the single protopore. Since the affinity of CPB for open WT pores is extremely low, we cannot decide in this case if it acts also as an open pore blocker. However, the experiments with the mutant K519E strongly support this interpretation. CPB block may become a useful tool to study the pore of ClC channels. As a first application, our results provide additional evidence for a double-barreled structure of ClC-0 and ClC-1.

KEY WORDS: ClC • slow gate • double barreled • anion channel • clofibric acid

INTRODUCTION

Ion channel research has profited greatly from the existence of specific high affinity antagonists of ionic permeabilities. Unfortunately, only a few specific blockers exist for Cl^- channels. Most "classical" Cl^- channel inhibitors, like DIDS, anthracene-9-carboxylic acid (9AC),* and others, act rather unspecific and often only at elevated concentrations (Nilius et al., 1999). For the Cl^- channels of the ClC family (Jentsch et al., 1999; Maduke et al., 2000) the situation is not much better, but promising results have been reported for the muscle chloride channel ClC-1, whose currents are strongly depressed by 9AC (Steinmeyer et al., 1991), and by the structurally quite different 2-(*p*-chlorophenoxy) propionic acid (CPP) and derivatives of it (Aromataris et al., 1999; Pusch et al., 2000). The inhibitory effect of CPP on the resting chloride conductance of skeletal muscle (gCl), largely mediated by ClC-1, has been intensively studied (De Luca et al., 1992a,b; Conte Camerino et al., 1988). Interestingly, the S(−) enantiomer of CPP has a much stronger effect on gCl than the R(+) enantiomer of these chiralic compounds. More recently, CPP was tested also on cloned rat (Aromataris et al., 1999) and

Address correspondence to Michael Pusch, Istituto di Cibernetica e Biofisica, Consiglio Nazionale delle Ricerche, Via de Marini 6, I-16149 Genova, Italy. Fax: 39-0106475-500; E-mail: pusch@barolo.icb.ge.cnr.it

*Abbreviations used in this paper: 9AC, anthracene-9-carboxylic acid; [Cl]e, extracellular [Cl]; [Cl]i, intracellular [Cl]; CPB, 2-(*p*-chlorophenoxy) butyric acid; CPP, 2-(*p*-chlorophenoxy) propionic acid; DIDS, 4,4′-diisothiocyanostilbene-2,2′-disulfonic acid.

J. Gen. Physiol. © The Rockefeller University Press • 0022-1295/2001/07/45/18 $5.00
Volume 118 July 2001 45–62
http://www.jgp.org/cgi/content/full/118/7/45

human (Pusch et al., 2000) ClC-1. In agreement with the previous studies, the S(−) enantiomers were found to be much more effective also on the cloned channel (Aromataris et al., 1999). In addition, the effect of CPP was shown to be strongly voltage-dependent, decreasing drastically at positive voltages, and the measurements on cloned channels allowed to demonstrate that CPP acts only from the cytoplasmic side. Testing CPP on several other members of the ClC family, we found that among the members tested only the homologous *Torpedo* channel (ClC-0) is blocked similarly to ClC-1, albeit with lower affinity (Pusch et al., 2000).

The voltage-dependent inhibition by S(−)-CPP (from now on simply called CPP) has been phenomenologically described as a "shift" of the $p_{open}(V)$ curve to more positive voltages (Aromataris et al., 1999) but its mechanism remains so far unclear. Unfortunately, ClC-1 has a relatively complex gating pattern (Rychkov et al., 1996, 1998) and its single-channel conductance is very low (Pusch et al., 1994; Wollnik et al., 1997; Saviane et al., 1999). Therefore, it is not an easy task to study the mechanism of CPP inhibition on this channel. The study of the similar inhibition of the homologous channel ClC-0 (Pusch et al., 2000) has several advantages since ClC-0 has a much larger single-channel conductance, slower gating kinetics, and less complicated selectivity properties (Miller, 1982; Chen and Miller, 1996; Rychkov et al., 1996, 1998; Ludewig et al., 1997a,b; Pusch et al., 1997). The gating of ClC-0 strongly suggests a "double-barreled structure" likely shared by ClC-1: both channels are most likely homodimers, and each subunit seems to form a separate pore that is rapidly gated independently from the other, whereas a slower gating mechanism regulates both pores simultaneously. Single-channel traces indeed show bursts of openings with two equally spaced conductance levels. The vastly different time scale of the two gating mechanisms of ClC-0 allows their separation on the macroscopic and on the single-channel level (Ludewig et al., 1996; Middleton et al., 1996). The double-barreled structure was recently strongly supported by direct structural data of a prokaryotic ClC-channel (Mindell et al., 2001). A double-barreled structure suggests at least two alternative mechanisms of channel inhibition by CPP. The drug could hinder the opening or block the permeation of single protopores; alternatively, it could hinder the opening of the slow common gate or block a pathway common to both protopores.

Recently Lin et al. (1999) described a single point mutation (C212S) that eliminates the slow gating process of ClC-0 leaving the common gate permanently open. At the single-channel level, no long closures of both pores could be detected. This mutant allows the study the of action of CPP independently of its possible effects on the slow common gate.

In the present study, we investigated in detail the mechanism of action of a derivative of CPP, 2-(*p*-chlorophenoxy)butyric acid (CPB), that inhibits with almost equal potency both the WT ClC-0 and the slow gate–deficient mutant C212S. From single-channel recordings, we conclude that CPB acts by inhibiting independently the two single protopore conductances, and not by favoring or re-enabling the closure of a common permeation pathway. Furthermore, our analysis of the [CPB]- and voltage dependence of macroscopic currents suggests that, besides hindering the opening of single protopores, CPB binding is also blocking pore permeation, consistently with the peculiar feature of chloride channels of having strongly correlated gating and conduction mechanisms. The voltage dependence of CPB inhibition results from a much lower affinity of open protopores for the binding of CPB, which is strongly destabilized by permeant chloride ions.

A single-pore structure has been proposed for ClC-1, based on results of substituted cysteine accessibility and macroscopic current measurements (Fahlke et al., 1998). However, single-channel measurements also show that ClC-1 channels have two equally distant conductance levels statistically distributed as expected from a double-barreled structure (Saviane et al., 1999). These results, together with considerations of structural homology and similarity of functional properties, indicate that ClC-0 and ClC-1 share the same architecture. Therefore, the model of Fahlke et al. (1998) for ClC-1 would predict that, in both ClC-1 and ClC-0, the equally spaced conductance levels observed in single-channel recordings are subconductance states of a single conduction pore. Our finding that CPB inhibits single protopore conductances is fully consistent with the CPB inhibition of physically distinct, independent conduction pathways, while being hardly interpretable in the context of a single pore structure. This adds further support to the already strong evidence for a double-barreled structure of ClC channels (Maduke et al., 2000; Mindell et al., 2001). Based on our results, CPB appears as a promising tool to investigate the structure of ClC-channels despite its low affinity.

MATERIALS AND METHODS

Molecular Biology and Oocyte Expression

The point mutant C212S of ClC-0 (Lin et al., 1999) was expressed in *Xenopus* oocytes as previously described (Pusch et al., 2000). The additional mutation K519E (Pusch et al., 1995; Ludewig et al., 1997a) was introduced in C212S by replacing the region of the C212S construct between the restriction sites BstEII (Promega) and BsiWI (New England Biolabs; containing the base triplet coding for residue 519) that of the corresponding region of the K519E construct. Since there is another BstEII cutting site downstream of the BsiWI site, we additionally used the MluI site (of the

vector) for a three piece ligation. The final construct was sequenced over all restriction sites used and over both mutations.

Electrophysiology and Solutions

For patch-clamping, the vitelline membrane of the oocytes was removed manually after incubation in hypertonic medium. Patch-clamp experiments were performed using the inside-out or outside-out configuration using an EPC-7 amplifier (List). The solutions had the following composition: the standard intracellular solution contained (in mM) 100 NMDG-Cl, 2 $MgCl_2$, 10 HEPES, and 2 EGTA at pH 7.3; the standard extracellular solution contained 100 NMDG-Cl, 5 $MgCl_2$, and 10 HEPES at pH 7.3. In the solutions with lower Cl^- concentrations, Cl^- was replaced by glutamate. Liquid junction potentials (<10 mV) were not corrected for. Solutions were changed by a perfusion system consisting of 4 tubes of ~200 μm diameter in which the tip of the patch pipette was inserted. The S(−) enantiomer of CPB was prepared as described by Pusch et al. (2000).

Data Analysis

Open probability curves were obtained as described previously (Ludewig et al., 1997a,b; Pusch et al., 1997, 2000). In brief, initial tail currents at a constant test voltage of −100 mV were measured after prepulses to various voltages and fitted by a Boltzmann function with "offset" of the form

$$I(V) = I_{min} + (I_{max} - I_{min})/1 + \exp(zF(V_{1/2} - V)/RT), \quad (1)$$

where I_{max} is the tail current after large prepulse depolarizations, z is the apparent gating charge, $V_{1/2}$ is the voltage of half-maximal activation, and I_{min} is a constant offset. The apparent open probability, $p_o(V)$, was obtained as the ratio $I(V)/I_{max}$; the residual open probability at negative voltage, p_{min}, was calculated as $p_{min} = I_{min}/I_{max}$. It reflects the (extrapolated) fraction of channels that do not close even at very negative voltages.

Single-channel analysis was performed as described by Saviane et al. (1999). Dwell time distributions were fitted by a maximum likelihood criterion taking all events into consideration without any binning.

Model Fitting

The kinetic model (Scheme IV) was fitted to the macroscopic experimental data using the procedure described below. For a given set of parameters defining the rate constants, the predictions of the model for the unbound probability $p_U(V)$ (Fig. 9) and the slow time constant τ_s (see Fig. 10) were calculated. $p_U(V)$ is simply the sum of the steady-state probabilities of unbound pores that are either in the closed or in the open state, p_C and p_O, respectively. Since it comprises four states, the model predicts three time constants for gating relaxations, whereas only two time constants, τ_f and τ_s, could be distinguished experimentally. However, we found that for parameters that described the unbound probability reasonably well, only two of the time constants predicted for the relaxations in the actual experimental conditions had a significant weight, one of them being like τ_f independent of CPB concentration (i.e., representing the normal gating kinetics) and a much larger one that was identified with τ_s.

The badness, b, of the model fitting of the data was calculated as:

$$b = \sum(p_U^{meas} - p_U^{fit})^2/\sigma_{pU}^2 + \sum(\tau^{meas} - \tau^{fit})^2/\sigma_\tau^2,$$

where $p_U{}^{meas}$, $p_U{}^{fit}$, and σ_{pU} are the measured and fitted values of p_U and the SEM of the measurement of p_U; τ^{meas}, τ^{fit} and σ_τ are the measured and fitted values of τ_s and the SEM of the measurement of τ_s, respectively. The quantity *b* was minimized using the simplex algorithm. To reduce the number of free parameters of the model, we made the following assumptions as is also described later in the text. First, we assumed that CPB stabilized the closed state mainly through a reduction of the opening rate, α', whereas the closing rate β' was set identical to β, which is the closing rate of unbound channels. Second, we assumed exponential voltage dependence of all rate constants, apart from the opening rate, α, that was calculated as described below. Third, we assumed that binding and unbinding of CPB to open channels was only slightly voltage-dependent with an apparent gating valence of −0.15 in accordance with the results obtained with the mutant C212S/K519E. Fourth, we imposed microscopic reversibility at the reversal potential for Cl^-. From this condition, we calculated the off rate constant from the open state at 0 mV, $k_{off}{}^O(0)$ as a function of the other rate constants. Fifth, the opening rate, α, and closing rate, β, of CPB-free channels were determined from the open probability, p_o, and the gating time constant, τ_f. The voltage dependence of p_o could be well described by a Boltzmann function with an offset:

$$p_o = p_{min} + (1 - p_{min})/(1 + \exp(zF(V_{1/2} - V)/RT)), \quad (2)$$

with $p_{min} = 0.092$, $V_{1/2} = -90$ mV, and $z = 0.96$ (data not shown).

The voltage dependence of β for the C212S channels was assumed to be of the same simple form derived from single-channel data (Chen and Miller, 1996) of the ClC-0 wild type:

$$\beta = \beta_o \cdot \exp(z_\beta FV/(RT)). \quad (3)$$

The parameters β_0 and z_β where determined by fitting τ_f data according to the relation:

$$\tau_f = (1 - p_o)/\beta, \quad (4)$$

yielding $\beta_0 = 6.8\ s^{-1}$, $z_\beta = -0.36$ (see Fig. 10, solid line). The opening rate, α, was consequently determined as:

$$\alpha = \beta \cdot p_o/(1 - p_o). \quad (5)$$

Model calculations were performed by standard numerical methods implemented in Visual C++. The parameters obtained from the fits are listed in Table I. For the fit, the four parameters marked with an asterisk in Table I were allowed to vary.

RESULTS

Effect of CPB on a Slow Gate–deficient Mutant of ClC-0

Like for ClC-1 (Pusch et al., 2000), only the S(−) enantiomer of CPB inhibited significantly the currents mediated by WT or mutant ClC-0 channels. CPB was effective only when applied from the cytoplasmic side, and its potency was similar to that of the propionate variant CPP (data not shown). To study the effects of CPB on the fast single-protopore gate of ClC-0, independently of possible effects related to the slow common gate, our present work deals exclusively with the mechanism of inhibition by CPB of the mutant C212S of ClC-0 that has been described by Lin et al. (1999). In this mutant,

TABLE I

Parameters Used for the Simulation of Scheme IV

	Standard condition	low [Cl]i	low [Cl]
$k_{on}^{C}(0)$	1.3*	3*	
z_{on}^{C}	−0.15*		
$k_{off}^{C}(0)$	2.2*	6*	
z_{off}^{C}	0.15		
$k_{on}^{O}(0)$	1.3	3	
z_{on}^{O}	0		
$k_{off}^{O}(0)$	326	418	231
z_{off}^{O}	0.15		
β_0	6.8	27	
z_β	−0.36		
β'_0	6.8	27	
$z_{\beta'}$	−0.36		
α'_0	1.5*		0.8*
$z\alpha'$	0.6		

Rate constants have the general form $r = r(0) \cdot \exp(z_r \cdot VF/(RT))$. The values at 0 mV are given in seconds^{-1} (the "on" rate constants are in millimolar^{-1} seconds^{-1}). Parameters that were used as free parameters in the fit are indicated by an asterisk. Blank fields indicate that the value was identical to that of the standard condition. The experiments in which the external chloride concentration was changed were obtained from outside-out patches, and the parameters $k_{on}^{C}(0)$ and $k_{off}^{C}(0)$ were slightly changed to 1.6 mM^{-1} s^{-1}and 2.5 s^{-1}, respectively, to better fit the response in high chloride.

the slow common gate appears to be constantly open, whereas the fast gate is practically identical to that of WT ClC-0. Fig. 1 A shows inside-out patch recordings of macroscopic currents carried by the mutant in the ab-

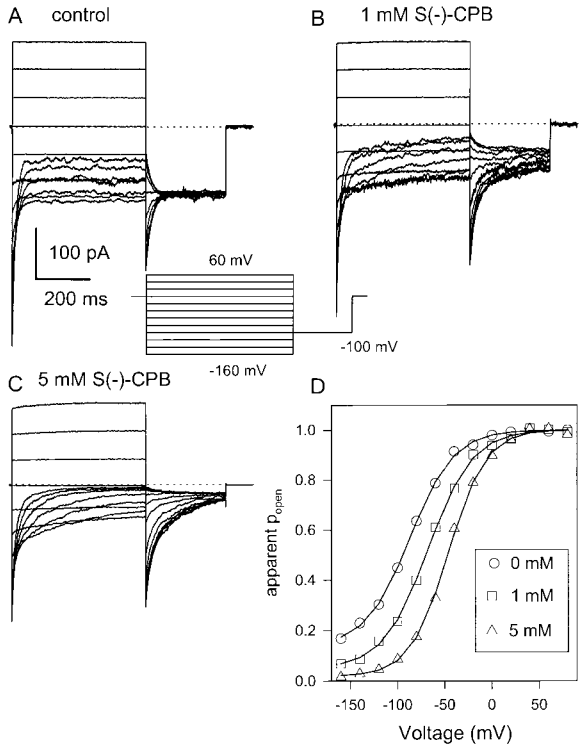

FIGURE 1. Qualitative effects of S(−)-CPB on the ClC-0 mutant C212S. (A–C) Family of voltage clamp traces recorded from one inside-out patch expressing the point mutant C212S of ClC-0. Currents were elicited using the pulse protocol shown in the inset. The concentration of intracellularly applied S(−)-CPB is indicated. (D) The apparent open probability (symbols) obtained from the initial current at the −100 mV tail pulse (see MATERIALS AND METHODS) together with fits of Eq. 1 to the data (solid lines).

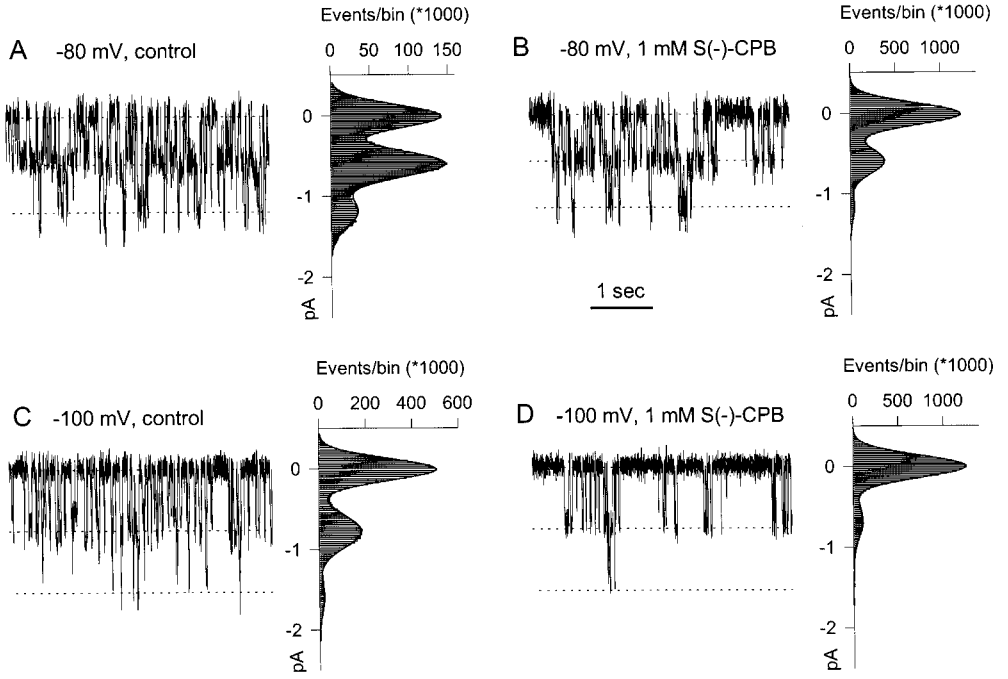

FIGURE 2. Inhibition of single protopores. A single C212S channel present in an inside-out patch was measured at a holding potential of −80 mV (top traces) and −100 mV (bottom traces) in the absence (left traces) and presence (right traces) of 1 mM S(−)-CPB. Only short stretches (4.3 s) of longer recording periods (>60 s for the recordings in the presence of CPB) are show for each condition. Next to each trace is shown (on the same current scale as the current trace) an amplitude histogram of the complete recording together with a fit of the sum of three Gaussian components. The peaks of the Gaussian fits are indicated as dashed lines on the current traces. The respective area of each Gaussian component was used to calculate the relative open probability of each conductance state (see Saviane et al., 1999) plotted in Fig. 3. Solutions are given in MATERIALS AND METHODS. Traces were filtered at 1 kHz for the analysis.

sence of CPB. The currents elicited by voltage steps from a holding potential of 0 mV have a fairly linear voltage dependence for positive voltages, indicating that most channels are open at 0 mV, whereas at negative voltages they display the typical ClC-0 fast deactivation that is well described by a single exponential function (Lin et al., 1999). Deactivation is not complete even at the most negative voltage applied (−160 mV). The initial tail current at the constant tail potential (−100 mV) reflects the apparent open probability at the end of the conditioning pulses (Pusch et al., 1995; Ludewig et al., 1997a; Fig. 1 D, circles), that can be well fitted by a Boltzmann distribution with an offset (Eq. 1). Applying CPB to the internal side of the patch (Fig. 1, B and C) has a barely appreciable effect on the outward currents elicited for $V > 0$, whereas the inward steady-state currents are reduced, with a stronger effect at more negative voltages and higher CPB concentrations, causing a reduction of p_{min} and a positive shift in the apparent $p_o(V)$ curve (Fig. 1 D). The decrease of the inward currents below control values introduces in the deactivation time course a slow component that probably reflects the onset of a CPB inhibition that is absent at positive voltages. The first question we address in this work is how such inhibition affects the apparent double barrel behavior of single C212S channels.

Single-channel Analysis of CPB Inhibition

CPB Acts on Single Protopores. CPB could inhibit the permeation of the single protopores of the double-barreled channel, or it could somehow shut down the conduction of both protopores simultaneously; e.g., by blocking a common pathway or by overcoming and reversing the effect of the C212S mutation and keeping the slow gate of ClC-0 closed. This question can be answered by single-channel recordings such as those illustrated in Fig. 2. The figure shows short stretches of recordings of a single C212S channel at −80 mV (top traces) and −100 mV (bottom traces) in the absence of CPB (left traces) and with 1 mM CPB present (right traces). The double-barreled appearance of the channel is evident by the presence of two equally spaced nonzero current levels that are never observed singly (see also Lin et al., 1999). CPB clearly decreases the mean time spent by the channel in any of the two conductive states, but it has no significant effect on their conductance (Fig. 2, dashed lines). From the latter observation, we can conclude that on-off kinetics does not cause flickering on the time scale of channel openings, i.e., the drug is not a fast open-pore blocker. Both in the absence and in the presence of CPB, the amplitude histograms of the recordings (shown next to the traces) could be well fitted with the sum of three Gaussian distributions from which the occupation probabilities of the three conductance levels, p_0, p_1, and p_2, were obtained (Fig. 3, bars). In the absence of CPB, these could be very well approximated by a binomial distribution of the form:

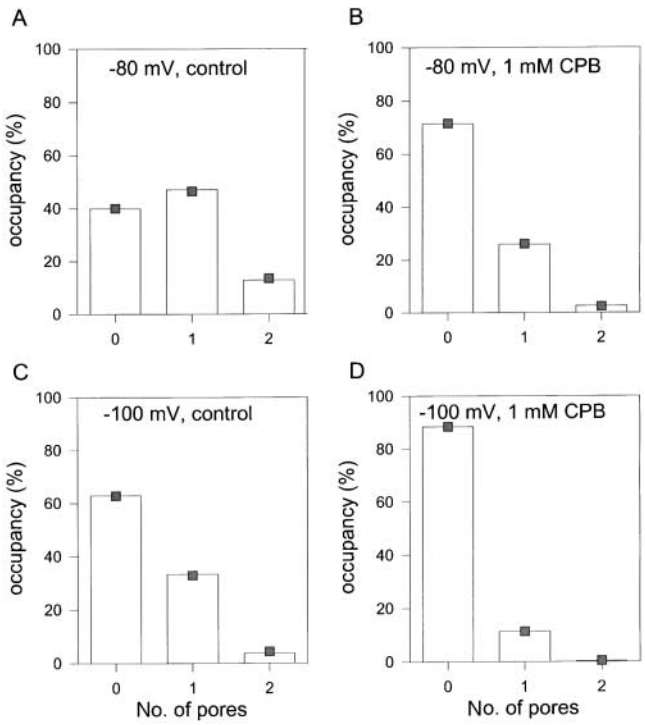

FIGURE 3. Binomial analysis of the single pore block. The occupancy of each of the three conductance levels (0, 1 "pore" open, 2 "pores" open) obtained from the Gaussian fits of Fig. 2 ([A] V = −80mV, no CPB; [B] V = −80 mV, 1 mM S(−)-CPB; [C] −100 mV, no CPB; [D] −100 mV, 1 mM S(−)-CPB). The squares in each graph indicate the best fit assuming an independent gating of two identical protopores according to Eq. 6 ([A] p = 0.37; [B] p = 0.15; [C] p = 0.21; [D] p = 0.06). Mean values ($n \geq 3$, ±SD) were as follows: for −80 mV, 0 CPB, p = 0.41 ± 0.03; for −80 mV, 1 mM CPB, p = 0.19 ± 0.03; for −100 mV, 0 CPB: p = 0.25 ± 0.03; for −100 mV, 1 mM CPB, p = 0.09 ± 0.02; for −120 mV, 0 CPB, p = 0.18 ± 0.01; and for −120 mV, 1 mM CPB, p = 0.05 ± 0.01.

$$\begin{aligned} p_0 &= (1-p)^2 \\ p_1 &= 2p(1-p) \\ p_2 &= p^2, \end{aligned} \qquad (6)$$

as expected if the measured current arises from the random openings of two independent pores with open probability p = 0.37 at −80 mV and p = 0.21 at −100 mV (Fig. 3, A and C, squares). Also in the presence of CPB, the occupation probabilities could be very well described by a binomial distribution (Fig. 3, B and D, squares, also see legend), but using reduced single-pore open probabilities, $p' = 0.15$ at −80 mV and $p' = 0.06$ at −100 mV. This result strongly supports the idea that CPB acts independently on single protopores, because if CPB prevented the opening or the permeation of both pores simultaneously, the probability distribu-

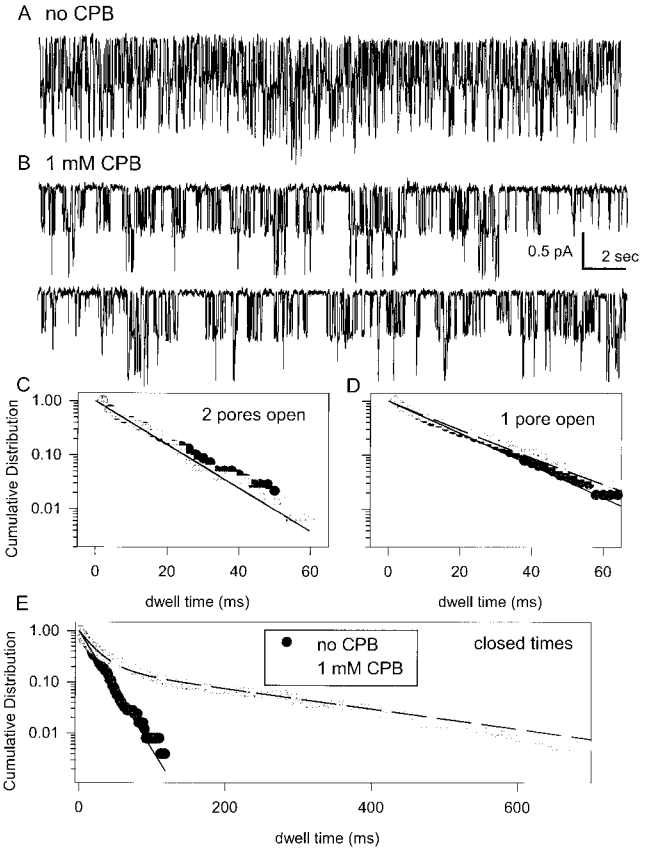

FIGURE 4. Kinetic analysis of a single channel at −80 mV. The long recordings shown in A (control) and B (with 1 mM CPB in the bath solution; from the same patch) were subjected to idealization after filtering at 500 Hz as described by Saviane et al. (1999). Traces were filtered at 50 Hz for display. Dwell times of the three conductance levels were fitted with a maximum likelihood procedure (Saviane et al., 1999). In the absence of CPB dwell times (C–E, circles) could be well fitted with single exponential functions (double open levels, [C] τ_2 = 10.8 ms; single open levels, [D] τ_1 = 14.6 ms; closed times, [E] τ_0 = 18.8 ms; see solid lines). In the presence of CPB, the dwell distribution of the double open conductance level (C, squares) could be well fitted with a single exponential with the same time constant as in the absence of CPB. The dwell time distribution of the single conductance level in the presence of CPB (D, squares) was much better described by the sum of two exponential functions that were fixed at 14.6 and 23 ms, respectively, as described in *Kinetic Analysis of Single Channels*. The distribution of zero current epochs (E, squares) was fitted with the sum of three exponential functions (E, dashed line) where two of the time constants were fixed to 18.8 and 37.6 ms, respectively, as described in the text and a larger time constant was determined by the fit to 220 ms. Qualitatively similar results were obtained in two patches at −80, −100, and −120 mV.

tion would change quite differently. In that case, the current would be zero while the channel binds CPB, whereas the relative probability of the two current levels while the channel is drug-free would remain the same and so would the observed ratio, p_2/p_1. The experimental data are in strong contrast with this prediction: in the experiment of Fig. 2, in the absence of CPB, the estimated values of p_2/p_1 were 0.27 at −80 mV and 0.11 at −100 mV, whereas in the presence of 1 mM CPB, the corresponding estimates were 0.10 and 0.02. A more direct qualitative demonstration that CPB acts on single protopores is the observation under drug application of numerous relatively long epochs containing only openings to the low conductance level (Fig. 4 B). We interpret these epochs as periods during which only one of the two protopores is inhibited by CPB. The comparison with recordings from the same channel before CPB addition (Fig. 4 A) shows that their spontaneous occurrence in the unaffected channel has a vanishingly small probability, and a simultaneous effect of CPB on both protopores cannot explain their appearance.

Kinetic Analysis of Single Channels

We performed a kinetic analysis of the single-channel records at −80, −100, and −120 mV in the absence and in the presence of 1 mM CPB. Fig. 4 shows the results for a patch at −80 mV. The complete recording stretches used for the kinetic analysis are shown in Fig. 4 A (no CPB) and Fig. 4 B (1 mM CPB). From the traces, it can already be seen that the main qualitative effect of CPB is to introduce long closures that are not seen in the absence of CPB. We performed a quantitative dwell time analysis after idealization of the single-channel traces as described by Saviane et al. (1999). In the absence of CPB, all three dwell time histograms (double open level, single open level, and closed) could be well fitted with single exponential distributions with time constants: τ_2 = 10.8 ms (double open; Fig. 4 C, circles); τ_1 = 14.6 ms (single open; Fig. 4 D, circles); τ_0 = 18.8 ms (closed times; Fig. 4 E, circles). These values are in accordance with previous results (Chen and Miller; 1996; Ludewig et al., 1997b; Lin et al., 1999) and are related to the opening rate, α, and closing rate, β, of the protopore gate by:

$$\tau_2 = 1/(2\beta), \quad \tau_1 = 1/(\alpha+\beta), \quad \tau_0 = 1/(2\alpha). \tag{7}$$

These equations allow a check of consistency because α and β are overdetermined. From the values of τ_0 and τ_1, which are measured better than τ_2 from much larger samples of events, we estimate from the recordings of Fig. 4 at −80 mV: α= 26.6 s^{-1} and β= 43.2 s^{-1}. From these estimates, we predict τ_2 = 11.6 ms (from Eq. 7), in very good agreement with the measured value of 10.8 ms. As a further test of consistency, we verify that the quantity $\alpha/(\alpha+\beta)$= 0.38 coincides, as expected, with the single-pore open probability (p = 0.37) measured for the same experiment from the current-amplitude histogram (Figs. 2 A and 3 A).

In the presence of 1 mM CPB, the dwell times of the double conducting states were not significantly differ-

ent (Fig. 4 C, squares) indicating that the rate of entry into CPB-inhibited states is much smaller than the normal closing rate, β. The situation is more complex for the unit and zero conductance durations. If only one pore is conducting, the other could be either just regularly closed or in a long-lived inhibited state. Respectively, the duration of detectable single openings is expected to be governed by the normal escape rate ($\alpha+\beta$) and by the lower rate β. Indeed, the histogram of the unit conductance durations shows the presence of an additional larger time constant that is well approximated by $1/\beta = 23.1$ ms (Fig. 4 D, squares and dashed line). If both protopores are nonconducting there are three possibilities: (1) both protopores are CPB-free and closed, a configuration with the normal escape rate 2α; (2) only one protopore is normally closed and stays so for a mean time $1/\alpha$, whereas the other is inhibited by CPB and is very unlikely to become conductive in any comparable time; and (3) both protopores bind a CPB molecule, in which case the transition rate to a conductive state is expected to be twice the effective rate of CPB dissociation. Indeed, the cumulative histogram of zero current durations is very well fitted with the sum of three exponentials, with two time constants fixed to $1/(2\alpha)$ and $1/\alpha$, and a fitted additional time constant of ~220 ms (Fig. 4 E, squares and dashed line).

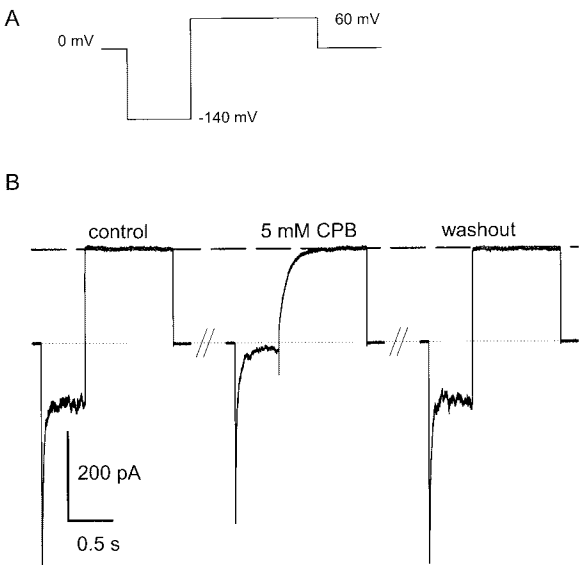

FIGURE 5. Complete unblock at positive voltages. To test if mutant C212S is slightly blocked by S(−)-CPB at positive voltages, a test pulse of the form shown in A was applied every 3 s. The intracellular solution of the inside-out patch was repeatedly switched between CPB-free and 5 mM S(−)-CPB containing solution. (B) The current responses after consecutive solution changes. The dashed line indicates the steady-state current level at 60 mV under all conditions. Clearly, the relief from inhibition at this voltage is practically complete. The dotted line indicates the zero current level.

Macroscopic Currents Analysis

The Removal of Inhibition at Positive Voltages Is due to CPB Dissociation. Our single-channel data show that between −120 and −80 mV the binding of CPB induces a long-lived nonconducting state of single independent C212S protopores, but leave open the question of whether CPB blocks ion permeation or decreases the opening probability of the protopore to which it is bound. Since single-channel recordings at much less negative voltages—where the switching of single drug-bound protopores to a conductive state might occur frequently enough and last long enough to be detected—are hampered by unfavorable signal to noise conditions, we have tried to answer this question by studying the voltage dependence of macroscopic current relaxations.

As shown qualitatively in Fig. 1, the inhibition of chloride currents by CPB concentrations as high as 5 mM is reduced by long depolarizations at large positive voltages. We demonstrated the total absence of a steady-state inhibition for $V \geq 40$ mV in experiments like that of Fig. 5. A pulse protocol comprising a 0.5-s pulse to −140 mV followed by a similar pulse to 60 mV and return to 0 mV (Fig. 5 A) was applied every 3 s to an inside-out macropatch and the perfusion was switched several times between control (no CPB) and test (5 mM CPB) solutions. Fig. 5 B shows a sample record before application of CPB, in the presence of 5 mM CPB and after washout. It is seen that with CPB the current decays to a much smaller value at the end of the pulse to −140 mV compared with the control situation, indicative of a strong steady-state inhibition at −140 mV. Vice versa, the current reaches exactly the same level of control at the end of the following 1-s pulse to 60 mV. Is this because CPB-bound pores can open at sufficiently depolarized voltages or because these voltages favor the full dissociation of CPB from the pores? The second interpretation is supported by the experiments illustrated in Figs. 6 and 7. Fig. 6 shows tail currents at $V_t = -100$ mV, after 700-ms prepulses to V_p from −160 mV to +120 mV, measured from the same inside-out patch before (A) and after (B) addition of 1 mM CPB to the normal perfusion solution. For clarity of illustration, only three of the records obtained for $V_p = -160$, −60, and +40 mV are displayed. The control records in A show the normal gating relaxations of C212S channels at −100 mV, which are very well described by a single exponential (smooth lines) with a V_p-independent time constant, τ_f, estimated in this experiment ~19.5 ms. On the other hand, the initial amplitude of the tail current, I_0, does depend on V_p, the relative amplitude of the following relaxation, $\Delta I_f / I_0$, being determined by the ratio of the steady-state open probabilities at $V = V_p$ and $V = V_t$. Therefore, the combination of τ_f and $\Delta I_f / I_0$ provides a hallmark for the currents mediated by the normal gating of unmodified channels. Measurements of $\Delta I_f / I_0$

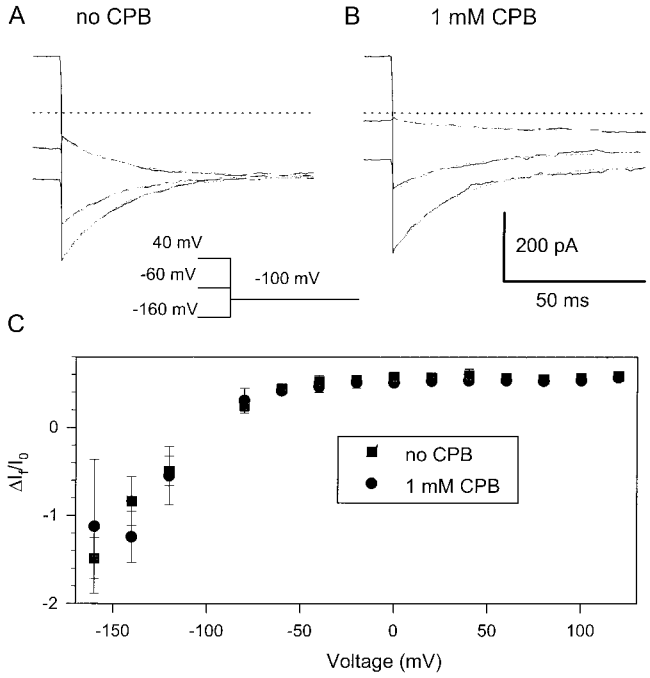

FIGURE 6. CPB-bound protopores do not contribute to steady-state conductances. The fast component of tail currents at −100 mV is used to identify the fraction of open pores that are drug-free at the end of a conditioning prepulse. Tail currents after prepulses of 700 ms duration to various voltages (traces are shown for −160, −60, and +40 mV) in the absence (A) and after addition of 1 mM CPB to the intracellular solution (B). The smooth lines in A are fits with single exponentials with the same time constant τ_f = 19.5 ms. The smooth lines in B are fits with double exponentials, comprising a fast component with the same time constant, τ_f = 19.5 ms, and a slower one, τ_s = 253 ms, equally independent of the prepulse. (C) The ratio $\Delta I_f/I_0$ of the amplitude of the fast exponential relaxation, ΔI_f, to that of the initial current, I_0, is plotted as a function of the prepulse voltage, both for CPB-free conditions (squares) and for 1 mM CPB (circles). (mean values ± SD, n = 4).

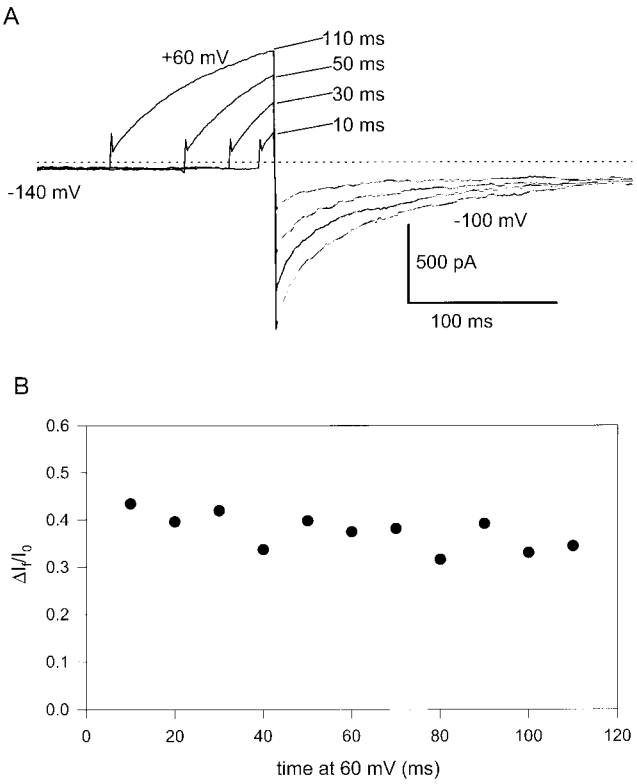

FIGURE 7. CPB-bound protopores are not conductive during recovery from inhibition. C212S channels in a patch exposed to 5 mM CPB were first maximally inhibited by a step to −140 mV for 2 s, the brought to +60 mV for variable times, T_p, and finally brought to −100 mV. The records shown in A, obtained for T_p = 10, 30, 50, and 110 ms, show a progressive decrease of the initial inhibition. However, the tail relaxation is in all cases a double exponential (smooth lines) with the same fast and slow time constants. (B) Plot of the relative amplitude of the fast relaxation, $\Delta I_f/I_0$, as a function of T_p; at all times during the removal of inhibition all conducting pores undergo fast relaxations as in the absence of CPB.

from four experiments are plotted as a function of V_p in Fig. 6 C as circles. The tail currents recorded in 1 mM CPB (B) need to be described by the sum of two exponentials (smooth lines), with a fast relaxation that has the same time constant of control, $\tau_f \sim$19.5 ms, and a slower component with a V_p-independent time constant, $\tau_s \sim$253 ms. Although it is obvious that the slow relaxation must reflect the interaction of the C212S protopores with CPB, the observation that is most important for the present argument is that the relative amplitude of the fast relaxation (Fig. 6 C) is not significantly different for any V_p from the respective quantity measured in CPB-free conditions. This implies that at the end of any prepulse all the conducting pores contributing to I_0 undergo the same fast relaxation toward the normal open-close distribution at $V = V_t$ as in drug-free conditions, i.e., they are all drug-free.

Also during the recovery from inhibition, it appears that no drug-bound hemichannels spend a significant time in a conductive state. This is shown by the experiment illustrated in Fig. 7. In the presence of 5 mM CPB, the C212S channels were first maximally inhibited by a pulse to −140 mV; the inhibition was then relieved to various extents by a pulse to +60 mV of variable duration, T_p, after which the voltage was stepped to −100 mV. Fig. 7 A shows records of the tail currents after 60-mV pulses with T_p = 10, 30, 50, and 110 ms, that reduced progressively the inhibition. In all cases, the tails were well fitted by a double exponential (smooth lines) with the same fast and slow time constants, and with the same relative amplitude of the fast relaxation (Fig. 7 B). The same result was obtained in four different patches and shows, by the same argument used in the discussion of Fig. 6, that drug-bound protopores do not spend even transiently any significant time in a conductive state.

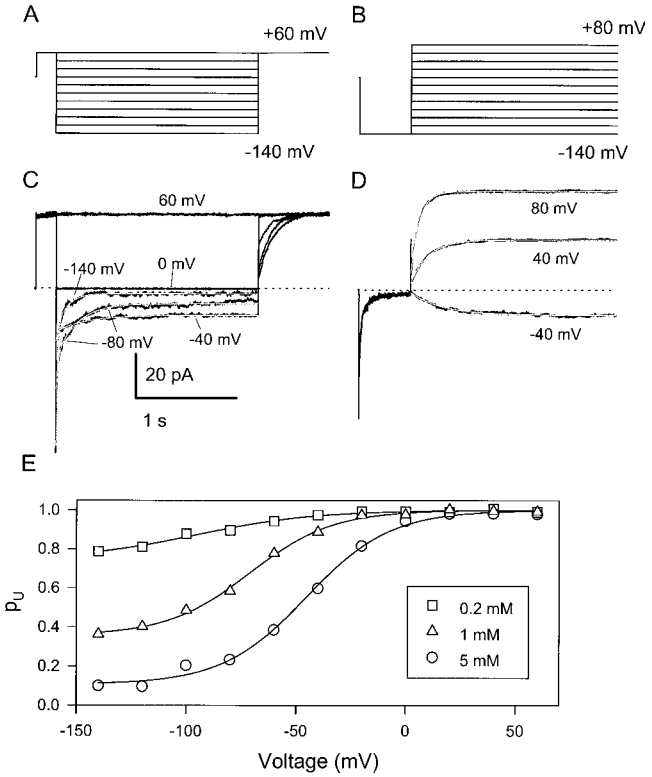

FIGURE 8. Study of the voltage dependence of CPB-inhibition. Two different pulse protocols are used to study the voltage dependence of on (A) and off (B) CPB inhibition. Recordings obtained from the same patch in 5 mM CPB with protocol A or with protocol B are shown in C and D, respectively. For clarity, only a few current traces are shown at the test voltages indicated. (C) After full removal by the prepulse to +60 mV, the on kinetics and steady-state level of CPB inhibition are measured for various steps to more negative voltages, V_p; the current relaxations at V_p are fitted by double exponential functions (smooth lines) with a fast time constant, τ_f, very close to that of normal deactivation, and a much larger time constant, τ_s, reflecting CPB-binding kinetics. At the onset of the following tail pulse to +60 mV, all the noninhibited channels open within ~1 ms (Accardi and Pusch, 2000), yielding an "instantaneous" current proportional to the unbound probability, $p_U(V_p)$. (D) After strong inhibition by a prepulse to −140 mV, the conductance increase for various steps to more positive voltages is fitted by a double exponential function for $Vp < -60$ mV and by a single exponential function for larger V_p's (smooth lines). (E) Shown the $pU = p_{unbound}$ values of the same patch shown in C for the single experiment using the pulse data shown in C. p_U was calculated as described in the text. The solid lines are fits of Eq. 1, and are shown only for clarity.

Voltage Dependence of CPB Binding Relaxations

The experiments discussed above show that both at large negative and at large positive voltages the interaction of the C212S channels with CPB is characterized by relatively slow relaxations of the macroscopic currents that are clearly distinct from the normal gating of drug-free channels. A quantitative dissection of the two processes is in fact possible at all voltages, and was performed using the two types of tail protocols illustrated in Fig. 8. In the first protocol (Fig. 8 A), the channels are first almost completely freed from inhibition and fully activated by a prepulse to +60 mV; they are then allowed to relax for 2 s toward their steady-state condition at a variable test potential, V_p. Finally, the voltage is stepped back to +60 mV. This protocol allows measurements of the voltage dependencies of CPB "on-binding" relaxations (during the conditioning to V_p) and of the steady-state CPB-binding probabilities (from the early currents after the last step to +60 mV; see below). Sample recordings obtained with this protocol from a patch exposed to 5 mM CPB are shown in Fig. 8 C. The second protocol (Fig. 8 B and sample recordings from the same patch are shown in Fig. 8 D) was designed to characterize "off-binding" relaxations. In this case, the channels were first almost maximally inhibited by a pulse to −140 mV, and then allowed to recover from inhibition at various more positive "tail" potentials.

The voltage dependence of the steady-state fraction of C212S channels that are not inhibited at a given CPB concentration can be estimated from the early currents after the last step to +60 mV in the pulse protocol of

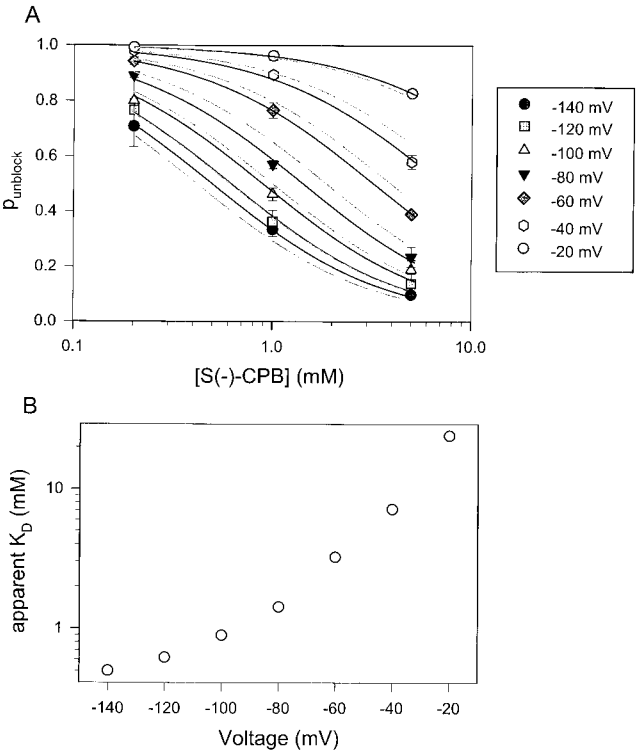

FIGURE 9. Steady-state binding of CPB to C212S protochannels. (A) Mean values of p_U are plotted versus the concentration of S(−)-CPB for the voltages indicated in the figure ($n \geq 4$ patches for each data point; error bars indicate SD). The solid lines are fits of Eq. 8 with the apparent dissociation constant, K_d, as free parameter at each voltage. The resulting K_d values are plotted in B as a function of voltage. The dashed lines were obtained from the simulation of Scheme IV with the parameters given in Table I.

Fig. 8 A. At this voltage, the channels that are drug-free at the end of the prepulse to V_p open completely within ~1 ms (Accardi and Pusch, 2000; see also τ_f data in Fig. 10) and contribute to an early current, $I_0(V)$, that appears almost "instantaneous" in comparison with the ~100-fold slower successive relaxation (Fig. 8 C). Therefore, the ratio:

$$p_U(V_p) = I_0(V_p)/I_\infty(+60),$$

where $I_\infty(+60)$ is the steady-state current flowing when all the channels are fully open at +60 mV, provides a fair estimate of the steady-state probability of channels being unbound at $V = V_p$. The values of $p_U(V_p)$ from the experiment of Fig. 8 are shown in Fig. 8 E at three different CPB concentrations. From these curves, the increase of the inhibition at negative voltages can be clearly seen. These data provide a more informative description of the increasing inhibition of the currents at negative potentials than those shown in Fig. 1 D. Most importantly they allow testing if such inhibition is consistent with a simple 1:1 binding of CPB. This consistency is shown by the plots of $p_U(V_p)$ estimates, obtained at any given V_p, as a function of CPB concentration, c (Fig. 9 A). At all voltages at which a significant block occurs ($V_p \leq -20$ mV), these estimates were well fitted by the simple titration function (Fig. 9 A, solid lines):

$$p_U(V_p,c) = 1/(1 + c/K_d(V_p)). \qquad (8)$$

The fitted K_d values are plotted in Fig. 9 B on a semilogarithmic scale as a function of voltage. It is seen that this apparent dissociation constant increases with voltage in the whole range from −140 to −20 mV, but much less steeply at increasing negative potentials. This rules out the simple idea that this voltage dependence arises solely from the movement of the charged ligand across a significant fraction of the transmembrane voltage upon binding. Some dependence of the binding on the channel state must also be involved.

The pulse protocol of Fig. 8 A allows also the study of the kinetics of the onset of CPB inhibition by following the decay of the currents after stepping the voltage from +60 mV to any $V_p \leq -20$ mV. As for the particular cases of Figs. 5–7, the example of Fig. 8 C shows that, at any V_p, this decay is well fitted (smooth lines in Fig. 8 C) by the sum of a fast exponential relaxation, with a time constant, $\tau_f(V_p)$, very close to that of normal deactivation, and a much slower component that has a roughly 10-fold larger time constant, $\tau_s(V_p)$, mainly reflecting the kinetics of the CPB-binding reaction. Measurements of $\tau_f(V_p)$ and $\tau_s(V_p)$, obtained with this protocol for various CPB concentrations, are plotted in Fig. 10 as solid symbols. Notice that, as stated above, the τ_f values do not show any dependence on CPB concentration and are not statistically distinguishable from the data in CPB-free conditions. In contrast, the τ_s values decrease with CPB concentration and we tentatively interpret them in the most simple way as time constants of a 1:1 binding relaxation:

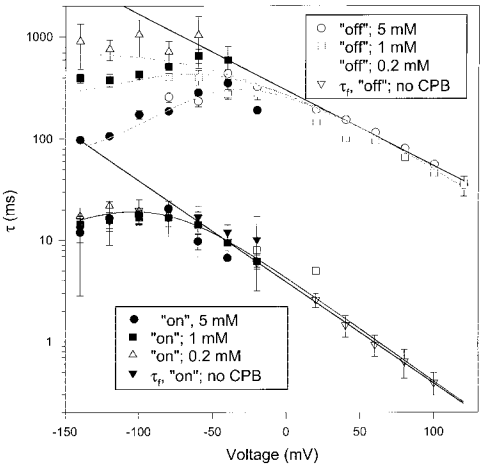

FIGURE 10. Kinetic analysis of macroscopic currents. Fast and slow time constants, τ_f and τ_s, were determined using the pulse protocols described in Fig. 8. Time constants obtained with the protocol of Fig. 8 A (i.e., with a positive prepulse) are indicated as "on" and plotted with filled symbols, whereas time constants obtained with the protocol of Fig. 8 B (i.e., with a negative prepulse) are indicated as "off" and plotted as open symbols. Each point is the mean of at least three determinations and the error bars indicate ±SD. The straight solid lines that fit the slow and the fast time constants in the positive voltage range have a steepness of a apparent gating valence of 0.43 for the slow time constants and a valence of 0.58 for the fast time constant, and illustrates the exponential voltage dependence of the time constants at positive voltages. The dashed lines were obtained by the simulation with Scheme IV (see MATERIALS AND METHODS). The solid line through the fast time constants is the least squares fit of Eq. 4, using Eqs. 2 and 3, obtained for $\beta_0 = 6.8\ s^{-1}$, $z_\beta = -0.36$.

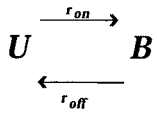

(SCHEME I)

where U denotes CPB-free channels in fast open-close equilibrium, B denotes nonconducting CPB-bound channels, and where the rates r_{on} and r_{off} are related to τ_s and to the unbound probability, p_U (Figs. 8 E and 9 A) by:

$$r_{on} = (1 - p_U)/\tau_s; \qquad r_{off} = p_U/\tau_s. \qquad (9)$$

According to our tentative interpretation, we expect r_{off} to be independent of, and r_{on} to be proportional to the CPB concentration, c:

$$r_{on} = k_{on} \cdot c; \qquad r_{off} = k_{off},$$

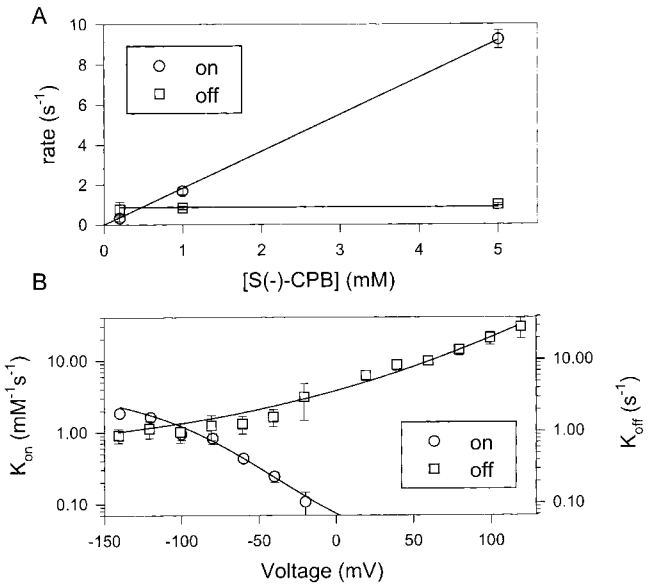

FIGURE 11. Kinetics of CPB association (on) and dissociation (off). The apparent rates of association, r_{on}, and dissociation, r_{off}, were calculated from the steady-state unbound probability, p_U, and from the slow time constants of current relaxations, τ_s, using Eq. 9. (A) Plots of mean values of r_{on} and r_{off} at −140 mV as a function of the CPB concentration, c; the straight lines are fits with $r_{off} = k_{off} = 0.88\ s^{-1}$ and $r_{on} = c \cdot k_{on} = c \cdot 1.84\ mM^{-1}s^{-1}$. (B) The apparent second order association rate constant, k_{on}, and first order dissociation rate constant, k_{off}, estimated as shown in A are plotted as a function of voltage (open symbols); For positive voltages, only k_{off} could be obtained as p_U is close to unity; the solid lines in B were obtained by the simulation with Scheme IV (see MATERIALS AND METHODS).

with k_{on} being the apparent second order association rate constant, and k_{off} the first order dissociation rate constant of the effective binding reaction. An example of such analysis, for $V_p = -140$ mV, is shown in Fig. 11 A where the plots of r_{on} and r_{off} as a function of c clearly reflect the consistency of the data with the above simple expectations. The same conclusion was reached from the analysis of "on" kinetics of CPB inhibition at any voltage in the range from −140 to −20 mV; plots of the resulting estimates of k_{on} and k_{off} as a function of V_p are shown in Fig. 11 B. Notice that the apparent k_{on} decreases with voltage much less steeply at large negative values than for $V_p > -80$ mV, where it decreases more than 10-fold for a 60-mV change. The voltage dependence of k_{off} is weaker than that of k_{on} in the whole range from −140 to −20 mV, but also the steepness of the increase of k_{off} with voltage tends to vanish at increasing negative voltages.

The apparent CPB-binding relaxations for $V_p \geq -80$ mV were studied with the protocol of Fig. 8 B. As for the on kinetics, also the decrease of the CPB inhibition induced by a conditioning prepulse at −140 mV is manifested by the presence of a much slower component in the time course of the current increase after the step to a more positive voltage (Fig. 8 D). Measurements of the two time constants, $\tau_f(V_p)$ and $\tau_s(V_p)$, obtained from the double exponential fit of these "tail currents" are plotted in Fig. 10 as open symbols. Notice that there is good agreement with the analogous on data (closed symbols), obtained with the other protocol described above, in the voltage range ($-80\ mV \leq V_p \leq -20$ mV) where both protocols could be used. Notice also that $\tau_s(V_p)$ is independent of c for $V_p > 0$. This is consistent with the above interpretation of τ_s, since at these voltages $p_U \sim 1$ (Figs. 8 E and 9 A) and τ_s is expected to be simply equal to the reciprocal of the first order dissociation rate constant, k_{off}. Accordingly, $1/\tau_s$ measurements for $V_p > 0$ are taken as k_{off} estimates and plotted as such in Fig. 11 B. This figure shows that the combined estimates of k_{off} from on and off measurements tend to increase exponentially for $V_p > -50$ mV, whereas they tend to a nonzero level at negative voltages.

Dependence of CPB Inhibition on Cl^- Concentrations

It is well-known that the fast gate of ClC-0 depends on the concentration of Cl^-, both extracellular ([Cl]e; Pusch et al., 1995; Chen and Miller, 1996) and intracellular ([Cl]i; Chen and Miller, 1996; Ludewig et al., 1997a). In general, the open probability increases with [Cl]e or [Cl]i. To gain information about the interaction of CPB with gating and/or permeation, it may be interesting to study the effects of changing chloride concentrations, since these changes are expected to affect both gating and the state of occupancy of sites in the permeation pathway that may be close or overlapping with the CPB binding site.

The Effect of Extracellular Chloride

To study the effect of [Cl]e on CPB inhibition, we used outside-out patches to allow a change of the extracellular solution. Fig. 12 A shows the effect of decreasing [Cl]e from 110 to 10 mM on the open probability of C212S channels in the absence of CPB. The $p_o(V)$ curve is shifted to more positive voltages by 38 ± 3 mV (mean ± SD), with little change in the asymptotic residual open probability at very negative voltages. The analysis of ClC-0 single-channel data (Chen and Miller, 1996) and our own estimates from macroscopic p_o and τ_f measurements according to Eqs. 4 and 5 (data not shown) indicate that the shift of the $p_o(V)$ curve is mainly due to a decrease of the opening rate, α, roughly by a factor of ~2.5 for $V \geq -100$ mV that tends to unity at more negative voltages, with little change in the closing rate, β. Fig. 12 (B–D) shows the effects of [Cl]e changes on the apparent values of the CPB-binding parameters, estimated as described above from p_U and τ_s measurements at various CPB concentrations. Qualitatively, all parameters, i.e., the apparent K_d, the effective on rate constant, k_{on}, and the effective off rate constant, k_{off}, are shifted to more positive voltages in low [Cl]e by the

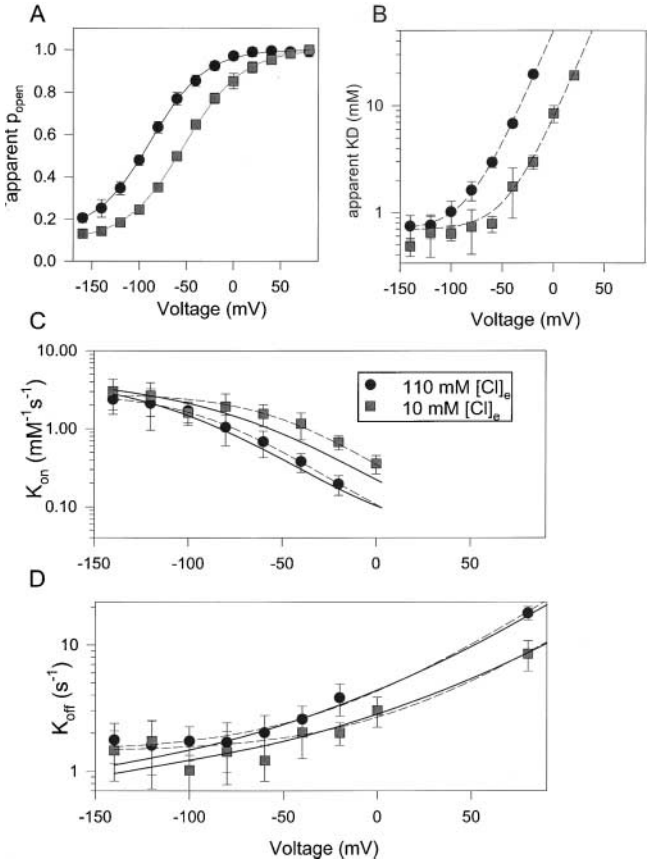

FIGURE 12. Effect of [Cl]e on the block. [Cl]e was changed from 110 mM (standard solution) to 10 mM (Cl^- was replaced by glutamate) on outside-out patches with no or with 5 mM S(−)-CPB present in the intracellular (pipette) solution. (A) The effect of this maneuver on the apparent open probability in the absence of CPB. The parameters of the fits (Eq. 1) are as follows: for high [Cl]e, $p_{min} = 0.13$, $V_{1/2} = -88.8$ mV, and $z = 0.95$; for low [Cl], $p_{min} = 0.08$, $V_{1/2} = -51.9$ mV, and $z = 0.79$. Using the analysis described for normal [Cl] the apparent K_d (B) and the effective on (C) and off (D) rate constants were determined as a function of voltage. The dashed lines in B–D were obtained in the following way: an arbitrary function was fitted to the data in high [Cl]e and the same function was replotted, shifted by 38 mV. Solid lines in C and D were calculated from a simulation of Scheme IV. The parameters were as in Table I, except that the values for $k_{on}^C(0)$ and $k_{off}^C(0)$ were adjusted slightly (see Table I legend).

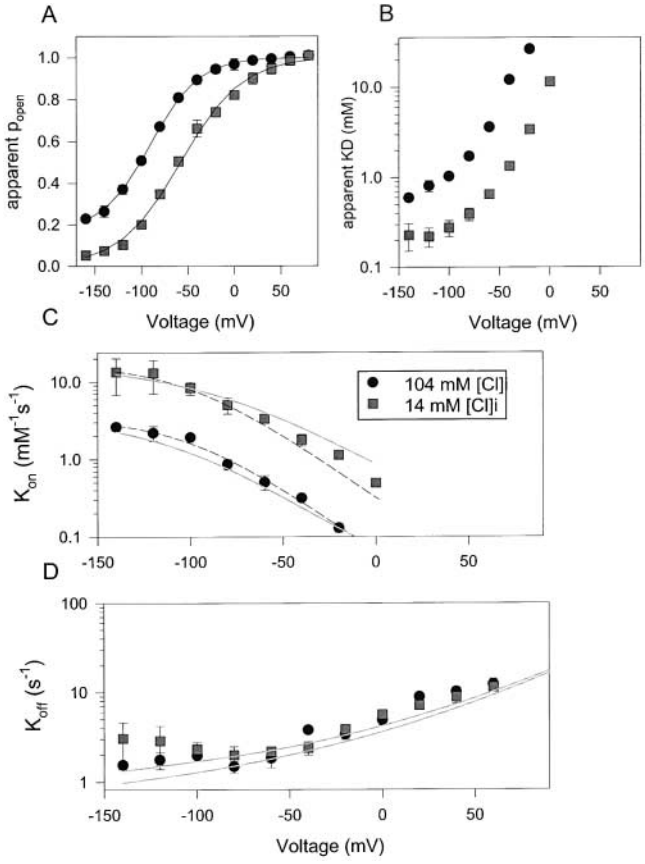

FIGURE 13. Effect of [Cl]i on the block. [Cl]i was changed from 104 mM (standard solution) to 14 mM (Cl^- was replaced by glutamate) on inside-out patches with no or with 1 mM S(−)-CPB present in the intracellular solution. (A) The effect of this maneuver on the apparent open probability in the absence of CPB. The parameters of the fits (Eq. 1) are as follows: for high [Cl]i, $p_{min} = 0.16$, $V_{1/2} = -90$ mV, and $z = 0.98$; low [Cl]i: $p_{min} = 0.04$, $V_{1/2} = -57.8$ mV, and $z = 0.94$. Using the analysis described for normal [Cl] the apparent K_d (B) and the effective on (C) and off (D) rate constants were determined as a function of voltage. The dashed line in C was obtained in the following way: an arbitrary function was fitted to the data in high [Cl]i and the same function was replotted, multiplied by a factor of five. Solid lines in C and D were calculated from a simulation of Scheme IV. The parameters were as in Table I.

same degree (38 mV) as the open probability in the absence of CPB (Fig. 12, B–D, dashed lines).

The Effect of Intracellular Chloride

In accordance with previous reports for ClC-0 channels (Chen and Miller, 1996; Ludewig et al., 1997a) we find that a reduction of [Cl]i from 104 to 14 mM shifts the open probability curve of the C212S mutant to more positive voltages and also strongly reduces p_{min}, as shown in Fig. 13 A. The analysis of ClC-0 single-channel data (Chen and Miller, 1996) and our own estimates from macroscopic p_o and τ_f measurements according to Eqs. 4 and 5 (data not shown) indicate that the main effect of lowering [Cl]i is an increase of the closing rate, β, by roughly a constant factor of approximately five. In the same figure are shown the effects of the [Cl]i change on the apparent values of the CPB-binding parameters, estimated as described above from p_U and τ_s measurements at various CPB concentrations. It is seen that both the apparent K_d and the effective on rate are changed by an almost constant factor of five (Fig. 13, B and C, dashed lines), whereas the off rate is practically unchanged by a reduction of [Cl]i (Fig. 13 D).

These results indicate that intracellular chloride ions antagonize the binding of CPB, either by competing for the same site or by occupying an inner site in the permeation pathway from which they destabilize CPB binding in a manner similar to that proposed for potas-

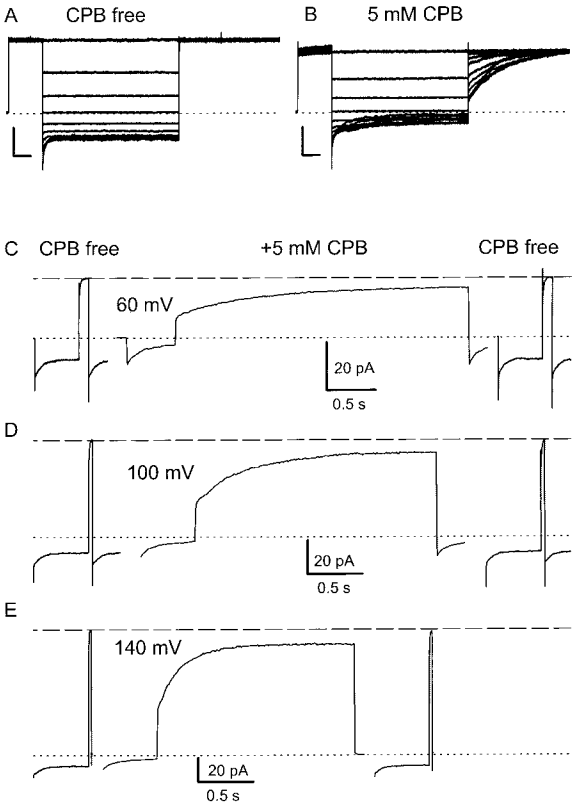

FIGURE 14. Open channel block of mutant K519E. Example traces of an inside-out patch without CPB (A) and with 5 mM CPB (B). The pulse protocol is as in Fig. 8 C, with longer pulse durations and a constant tail pulse to +60 mV. (C–E) Experiments analogous to those of Fig. 5 in which 5 mM CPB was repeatedly perfused and washed away. Note the incomplete relief from inhibition even at +140 mV. Bars indicate 0.5 s and 20 pA, respectively.

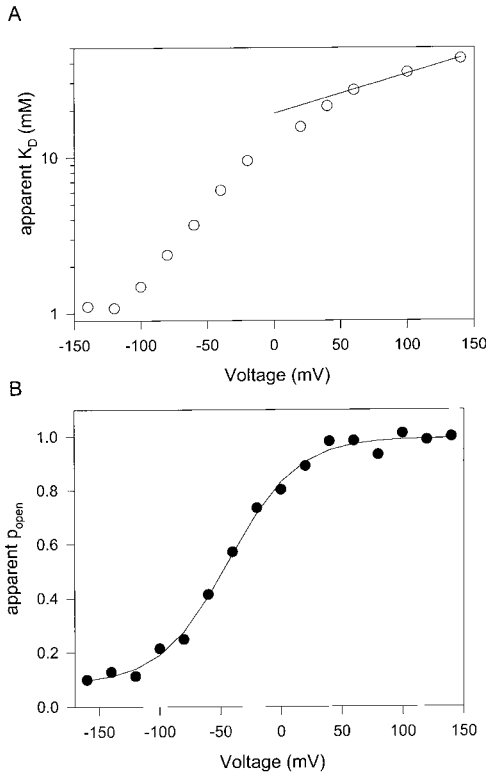

FIGURE 15. Voltage dependence of the block of mutant K519E. (A) From the mean values of the ratio of the steady-state current in presence and absence of CPB, I(CPB)/I(0), for CPB concentrations of 1, 5, and 10 mM the apparent dissociation constant, K_d, was obtained by a fit with Eq. 8 for voltages ranging from −140 to +140 mV. The resulting K_d values are plotted as a function of voltage. The straight line represents a fit of a simple exponential function of the points at 60, 100, and 140 mV. It has a slope corresponding to an apparent electrical distance of 0.15. (B) Apparent open probability of the fast gate of the mutant K519E in the presence of 5 mM CPB. After long saturating pulse to voltages between −140 and +140 mV, the currents recorded at the beginning of a pulse to −140 mV were normalized and plotted as a function of the prepulse voltage. The solid line is the Boltzmann fit obtained with Eq. 1 using parameters $p_{min} = 0.085$; $V_{1/2} = -43.0$ mV, and $z = 0.90$.

sium channels, in which peptide blockers are destabilized by K^+ ions (MacKinnon and Miller, 1988; Terlau et al., 1999).

Open Channel Block of the Mutant K519E

We investigated the effects of the mutation K519E on the CPB inhibition. We chose this mutation because amino acid 519 is probably located at the intracellular pore entrance of the channel (Middleton et al., 1996; Ludewig et al., 1997a) where most of our results suggest that CPB binding might occur. Mutant K519E has a reduced single-channel conductance, an outwardly rectifying instantaneous IV, and slower single protopore gating kinetics (Pusch et al., 1995; Middleton et al., 1996; Ludewig et al., 1997a). As for WT CLC-0, the additional C212S mutation eliminates the slow closing also in the K519E construct (not shown). Fig. 14 shows sample records of macroscopic currents obtained with the protocol of Fig. 8 A in CPB-free conditions (A) or after the addition of 5 mM CPB (B). It is also seen that the conductance of C212S-K519E channels is inhibited by CPB much more strongly at negative voltages, and that the relaxations of CPB at both positive and negative voltages are distinctly slower than the gating kinetics of these channels. However, we notice an important difference in that the relief from inhibition is not complete even at voltages as high as +140 mV (Fig. 14, C–E). Therefore, by studying the fractional decrease of conductance at various CPB concentrations (1, 5, and 10 mM) we were able in the case of C212S-K519E to estimate the apparent K_d for CPB binding in the full range of voltages from −140 to +140 mV.

From the fractional inhibition of steady-state currents at various concentrations of CPB, we derive the dissociation constant estimates shown in Fig. 15 A as a function of voltage. It is seen that K_d increases steeply with voltage between −100 and 0 mV but the dependence is much flatter at both ends of the voltage range. The af-

finity of the mutant is slightly smaller than that of WT at negative voltages but higher at positive voltages, where it is unmeasurable for WT (compare with Fig. 9 C). The values between +60 and +140 mV change with an equivalent valence of ~0.15 (Fig. 15 B, solid line).

Also, the kinetics of CPB effects are quite different for the double mutant C212S-K519E as compared with C212S, showing an interesting parallelism with differences in the gating kinetics of the two constructs. First, the relief from inhibition at positive voltages was significantly slower: τ_s= 1,000 ± 100 ms at +60 compared with the WT value of 115 ± 4 ms. Most interestingly, the ratio of the slow off time constant and the fast gating time constant, τ_s / τ_f, at +60 mV is ~100 for both WT and mutant (τ_f (mutant) = 10.2 ± 2.2 ms; τ_f (WT) = 0.93 ± 0.2 ms). Also the slow time constant at negative voltages that accompanies the onset of inhibition is larger in the mutant compared with WT (τ_s at 5 mM and −140 mV of the mutant K519E: τ_s = 590 ± 60 ms versus the WT value of 98 ± 5 ms). The ratio τ_s / τ_f is smaller at −140 mV, but again very similar for mutant and WT (τ_s / τ_f (mutant) ~ 6.6; τ_s / τ_f (WT) ~ 7.6).

The persisting inhibition at positive voltages, that is not seen with WT ClC-0, could be caused by three different mechanisms: (1) the maximal open probability of CPB-bound channels could be significantly smaller than one; (2) the open probability in the presence of CPB could be "shifted" very strongly; or (3) open channels could be directly blocked. The first possibility is unlikely because nonstationary noise analysis indicated a maximal open probability close to one (not shown). To distinguish between the latter possibilities, we measured the apparent open probability using the conventional tail current protocol (Fig. 15 C). The resulting apparent p_o (Fig. 15 D) clearly saturates for voltages ≥ +40 mV, indicating that the open probability in the presence of 5 mM CPB is maximal at these voltages where inhibition is substantial. The most likely explanation of these results is that CPB exerts an open channel block on the mutant and that the affinity of the open state is slightly voltage-dependent with an apparent valence of 0.15.

A Kinetic Model for CPB Inhibition

In all our measurements, for voltage steps between any two levels in the whole range from −140 to +140 mV, we observed macroscopic current relaxations described by single exponentials (no CPB) or double exponentials (with CPB) with time constants solely dependent on the final voltage level. This general feature, per se, is a strong indication that the independently gated protopores possess only two statistically significant states and that CPB binding only adds one significant state to this counting. Therefore, the most simple models that could describe our observations assume that CPB can either bind only to the open state, blocking ion permeation, or bind only to the closed state, preventing the opening transition:

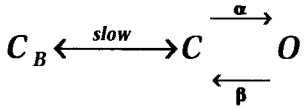

(SCHEME II)

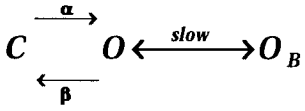

(SCHEME III)

In either one of the above models, the slow time constant of the single-channel closed state dwell time histogram or the slow component of macroscopic current relaxations would reflect the slow binding reaction of CPB to the appropriate protopore state. Both models are attractive for their simplicity and could be forced to fit the macroscopic and single-channel data for WT channels by choosing ad hoc voltage dependencies for the true association and dissociation rate-constants of CPB binding. However, both models predict that the measured k_{off} is the true first order dissociation rate constant of CPB unbinding, expected as such to have a simple exponential dependence on voltage, which is contrary to what is actually observed (Figs. 11 B, 12 D, and 13 D). Each scheme also has some other additional inconsistency with the data. Scheme II has the nice feature of predicting the steep decrease of k_{on} with voltage, as a mere consequence of the decrease of closed-pore probability even in the absence of an intrinsic voltage dependence of CPB association rate; but it is inconsistent with the residual block of C212S-K519E channels at very large voltages that drive all channels to the open-pore conformation. Vice versa, in Scheme III, the strong voltage dependence of k_{on} for V > −100 mV would reflect an intrinsic property of CPB association that is hardly reconcilable with its tendency to vanish at very negative voltages (Figs. 11 B, 12 C, and 13 C).

A logical complication of any of the above models is to assume that CPB can bind to both conformations of the protopores, resulting in a 4-state model (Scheme IV):

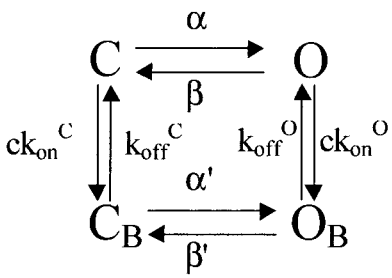

(SCHEME IV)

The binding properties of the closed state are clearly different from those of the open state and we know already that the gating is strongly influenced by CPB. The results of Figs. 6 and 7 and the results obtained with the mutant K519E indicate that the open bound state O_B is nonconducting, i.e., that CPB directly blocks the pore. The flattening out of the apparent on and off rates at negative voltages (Fig. 11) suggest that binding of CPB to the closed state is little voltage-dependent. The experiments with the mutant K519E also indicate that binding of CPB to the open state is little voltage-dependent; the valence of the open channel block of the mutant was estimated to be ~0.15. On the other hand, the effective rate of recovery from block at positive voltages shows a simple exponential voltage dependence with an apparent valence of ~0.43 for voltages up to 120 mV (Fig. 10). These properties strongly suggest that the recovery from block occurs through the state O_B and that the opening rate α' is rate limiting for this process. This implies that the off rate from the open state, k_{off}^O, is large compared with α' at all voltages tested here. This interpretation of the slow recovery from block at positive voltages is supported by the following two observations. First, recovery from block of the mutant K519E is slowed by a factor of ~10, practically by the same factor as the regular opening rate, α, in accordance with the hypothesis that the "opening" rate α' is reduced by the same factor in the mutant. Second, the reduction of extracellular chloride reduces the opening rate α and the effective off rate at positive voltages by about the same factor. On the other hand, the experiments with low intracellular chloride indicate that a reduction of the closing rate β, and, thus, likely also of the rate β', has almost no effect on the effective off rate constant (Fig. 13).

Therefore, we fitted the predictions of the model to the unblock probability, $p_U(V)$ (Fig. 9) and the slow time constants (Fig. 10) using the following simplifying assumptions in accordance with the above considerations. First, we assume that the rate β' is equal to β. Second, we fixed the voltage dependence of the off rate from the open and from the closed state to 0.15 and that of the on rate to the open state to zero. Third, we fixed the voltage dependence of α' to 0.6, according to the slope of the fast opening time constant at positive voltages (see Fig. 10). Fourth, we assumed that the on rate to the open state is identical to the on rate to the closed state.

The model was fitted to the $p_U(c, V)$ data (Fig. 9 A) and to the slow time constants (Fig. 10) as described in MATERIALS AND METHODS. The free parameters in the fit were: $k_{on}^C(0)$, $k_{off}^C(0)$, z_{on}^C, $\alpha'(0)$ (see Table I). The model allows a reasonable description of the macroscopic data (see dashed lines in Fig. 9 and 10 and solid lines in Fig. 11). The model captures the basic features of CPB inhibition that are experimentally observed. In the negative potential range, binding is relatively voltage-independent, and binding as well as unbinding steps occur primarily via the closed state; CPB binding strongly disfavors channel opening by reducing the opening rate, and vice versa the off rate from the open state is much larger than the off rate from the closed state, such that the affinity of the open state is very small. The latter two properties lead to the single exponential time course of the disinhibition at positive voltages.

Because of the difficulty in experimentally determining the K_d of the open state the parameters given in Table I are at best good guesses of the true values. Interestingly, caused by the large off rate from the open bound state, this state is only very little occupied. This implies that the model is practically equivalent to one in which the open bound state is conducting, i.e., a model in which CPB is a pure gating modifier.

What does the model predict under reduced chloride concentrations? Without CPB, the main effect of reducing [Cl]e is to decrease the opening rate α with little effect on β (Chen and Miller, 1996). Within our simple 4-state model it is therefore reasonable to assume that also the opening rate of CPB-bound channels, α', is reduced in low [Cl]e. Indeed, the data show that the apparent $k_{on}(V)$ curve is shifted as much as the $Po(V)$ curve and that the $k_{off}(V)$ at $V > -50$ mV (where unbinding occurs mainly via the $C_B \rightarrow O_B \rightarrow O$ pathway) is decreased by the same factor as α. The results of the experiments in low [Cl]e could indeed be reasonably well reproduced by just reducing the opening rate α' by a factor of approximately two (Fig. 13, D and E, solid lines, and parameters in Table I). This suggests that a reduction of [Cl]e has little direct effect on the state-dependent binding of CPB, the overall effect being only influenced by the [Cl]e dependence of the relative probability of the two conformational states of the channels.

The [Cl]i dependence of CPB inhibition is also nicely consistent with our simple model. The main effect of lowering [Cl]i is known to be an increase of the closing rate β (Chen and Miller, 1996). The apparent k_{off} reflects at negative voltages the true dissociation rate constant of CPB from closed channels, whereas at positive voltages it is mainly determined by α'. If the opening rate is not changed, we expect that k_{off} is not changed at any voltage, as indeed observed. On the other hand, the β increase at negative voltages is not expected to increase much the apparent k_{on}. In this range, the observed change of k_{on} is by a factor increasing from 5.5 to 9. The data are consistent with a main effect of competition between CPB and [Cl]i for the same binding site. Such competition would make:

$$k_{on} = k_1/(1 + [Cl]i/K_{Cl}).$$

Thus, this suggests that intracellular chloride strongly interferes with CPB binding.

DISCUSSION

On purpose, we have described our results for C212S channels by stating that CPB-bound pores do not contribute appreciably to the chloride conductance, rather than stating that CPB-bound pores cannot open, because we could not exclude from the experiments with this construct that the dissociation of CPB from the protopore to which it is bound occurs at positive voltages preferentially via the intermediate step of pore opening. What our data indicate is that the dwelling in such a "transition state" is unmeasurably short at our time resolution, so that whether this state is conductive or not has no practical consequence on the effect of CPB inhibition. However, distinguishing between these two possibilities has important consequences for the interpretation of the inhibition mechanism. In one case we would conclude that the binding of CPB is allosterically interacting with the portions of the protopores whose structural changes gate the opening of the pore. In the other, we would have a strong indication that CPB binds to a site where it acts as a pore blocker and this would be nicely consistent with the competitive interaction of CPB with the permeant chloride ions. The mutant K519E changes several properties of the channel, including conductance and gating kinetics. However, the basic properties are similar to WT and introduction of various amino acids at position 519 lead to gradual changes in channel properties (Middleton et al., 1996). Thus, it is very likely that the qualitative properties of the CPB-block seen for the mutant can be transferred to the WT. In particular, the mutant exhibits a clear inhibition at positive voltages providing evidence that, besides interfering with the gating transitions, CPB does indeed also block ion conductance. If this is the case, it might also be expected that changes of the extracellular Cl^- concentration affect the affinity for CPB in a manner similar to the effects of extracellular K^+ and TEA^+ on internal TEA^+ block of K^+ channels (Thompson and Begenesich, 2000), whereas here we found no direct effect of [Cl]e on CPB binding. However, because CPB preferentially binds to closed channels, the effect of extracellular Cl^- is expected to be small. Furthermore, even in the case of K^+ channels the effects of "contralateral" ions on block appear to be mediated indirectly and not through direct electrostatic repulsion (Thompson and Begenesich, 2000) and it cannot be expected that the same mechanisms are valid for Cl^- channels.

From our results, the following four basic conclusions can be drawn. First, CPB inhibits single protopores of the presumably double-barreled channel. Second, it binds preferentially to single protopores that have a closed fast gate. Third, the binding is influenced by internal Cl^- in a manner consistent with a competition between the two anions for the occupation of the same or a closely located site; and fourth, when binding to the open conformation of the pore, CPB probably blocks the pore permeation.

To what extent are these results evidence in favor of a double-barreled architecture of the channel? The single protopore inhibition clearly shows that there are two binding sites on the channel that are practically independent of each other. Furthermore, the properties of the inhibition by CPB strongly suggest that the block occurs within the ion conducting pathway. Taken together, our results strongly favor a double pore architecture of ClC-0, in agreement with the recent projection structure of a prokaryotic ClC channel (Mindell et al., 2001). The most intriguing property of CPB-block is that it can be overcome by sufficiently large voltages, that lead to channel opening. At a first glance, this behavior is reminiscent of that of a typical "gating-modifier": drug-bound channels are more difficult to open; therefore, in the presence of CPB the effective open probability curve is shifted to more positive voltages. In fact, this interpretation has been adopted by Aromataris et al. (1999) in their description of the effect of CPP on ClC-1. However, several quantitative properties are not in agreement with a simple gating modifier mechanism. First, whereas CPB induces long closed periods in single-channel recordings, proving the existence of a long-lived, drug-bound state, the open time distribution is not significantly affected, ruling out the presence of a long-lived liganded open state. Furthermore, a simple gating-modifier model would predict that the contribution of the fast decaying exponential component at negative voltages varies with the relative occupation of the liganded open state compared with the drug-free open state. In contrast, our analysis shows that a conductive drug-bound channel is unlikely to be occupied at any voltage to any significant extent. In addition, we found an open channel block for a point mutation, suggesting a similar mode of action also for WT.

An interesting property of the CPB block is that even though the kinetics can be well described by a simple bimolecular reaction, the association rate-constant is far below that of a diffusion limited process. This means that a large free-energy "barrier" separates the intracellular fluid from the binding site. This finding is actually again in accordance with the idea that the binding site of CPB lies within the conduction pathway. The strongest evidence in favor of a binding of CPB in the pore comes from the experiments with the mutant K519E. The partial inhibition at voltages up to 140 mV strongly suggests an open pore block. However, more experiments are needed to further nail down this conclusion.

Our data can be well described by a simple model in which the closed state has a much larger affinity or CPB than the open state and in which binding itself is only slightly directly voltage dependent. The slow relief from inhibition at positive voltages does not directly reflect the unbinding of CPB but is governed by the slower and rate limiting opening step of the drug-bound channels, α'. This small value of α' reflects the stabilization of the closed state by CPB. This interpretation is supported by the results with the mutant. Regular fast gating of mutant K519E is significantly slower than WT. The very slow relief from inhibition of the mutant results from a proportional slowing of the opening rate, α', of CPB-bound channels. The fact that also the apparent on rate at negative voltages is smaller in the mutant as compared with WT is more difficult to explain. One reason might be that the minimum open probability of the mutant is much larger than for WT (Pusch et al., 1995; Ludewig et al., 1997a), reducing the effective on rate.

The kinetic effects of mutation K519E on CPB unbinding appear to be largely caused indirectly by a slowed and otherwise changed gating kinetics of the mutant, and also the affinity of the mutant at negative voltages is not drastically changed. It is therefore unlikely that lysine 519 forms part of the binding site of CPB. We rather speculate that the binding site is further inside the pore, beyond the supposedly superficial location of K519.

The model can account quantitatively for the macroscopic measurements. Also the single-channel data are in good qualitative agreement with the model. Further single-channel measurements are needed, however, for a full comparison with the model.

The model is also in good agreement with our results obtained in low [Cl]e and [Cl]i. Whereas external Cl^- appears not to directly interact with CPB, lowering of intracellular Cl^- could be fitted only by adjusting mainly the on rates to the closed and open states. Based on this, we speculate that intracellular Cl^- directly interferes with CPB binding, either by competition for a common binding site or by the occupation of closely located interacting binding sites. More experiments are clearly needed to explore this aspect of CPB block in more detail. The apparently complicated effects of CPB on gating are not at all surprising if CPB does bind in the pore because it is known that the gating of ClC-0 is tightly linked to permeation. Any agent that impedes the access of chloride as a channel opener will have profound effects on gating.

In conclusion, even though the block by CPB of the point mutant C212S of ClC-0 is of rather low affinity, it allowed us to obtain additional evidence for a double-barreled architecture of the channel. Furthermore, the drug shows very interesting interactions with the gating state of the channel and its study may therefore yield important insights into channel function. In particular, it will be important to identify the CPB binding site. If future experiments cement the conclusion that CPB is a pore blocker, the regions of the primary structure participating in the binding site may give a hint to where the pore is located in ClC channels, viewing from the inside.

We thank Dr. T.Y. Chen for providing the mutant C212S of ClC-0.

The work has been supported by Italian CNR PS No. 98-3265-74 and 99.2312.74 and partially by Telethon Italy, grant No. 1079 to M. PUSCH.

Submitted: 9 April 2001
Revised: 18 May 2001
Accepted: 21 May 2001

REFERENCES

Accardi, A., and M. Pusch. 2000. Fast and slow gating relaxations in the muscle chloride channel CLC-1. *J. Gen. Physiol.* 116:433–444.

Aromataris, E.C., D.S. Astill, G.Y. Rychkov, S.H. Bryant, A.H. Bretag, and M.L. Roberts. 1999. Modulation of the gating of ClC-1 by S-(−)2-(4-chlorophenoxy) propionic acid. *Br. J. Pharmacol.* 126: 1375–1382.

Chen, T.Y., and C. Miller. 1996. Nonequilibrium gating and voltage dependence of the ClC-0 Cl^- channel. *J. Gen. Physiol.* 108:237–250.

Conte Camerino, D., M. Mambrini, A. De Luca, D. Tricarico, S.H. Bryant, V. Tortorella, and G. Bettoni. 1988. Enantiomers of clofibric acid analogs have opposite actions on rat skeletal muscle chloride channels. *Pflügers Arch.* 413:105–107.

De Luca, A., V. Tortorella, and D. Conte Camerino. 1992a. Chloride channels of skeletal muscle from developing, adult and aged rats are differently affected by enantiomers of 2-(*p*-chlorophenoxy) propionic acid. *Naunyn-Schmied Arch. Pharmacol.* 346:601–606.

De Luca, A., D. Tricarico, R. Wagner, S.H. Bryant, V. Tortorella, and D. Conte Camerino. 1992b. Opposite effect of enantiomers of clofibric acid derivative on rat skeletal muscle chloride conductance: antagonism studies and theoretical modeling of two different receptor site interactions. *J. Pharmacol. Exp. Ther.* 260:364–368.

Fahlke, C., T.H. Rhodes, R.R. Desai, and A.L. George, Jr. 1998. Pore stoichiometry of a voltage-gated chloride channel. *Nature.* 394: 687–690.

Jentsch, T.J., T. Friedrich, A. Schriever, and H. Yamada. 1999. The CLC chloride channel family. *Pflügers. Arch.* 437:783–795.

Lin, Y.W., C.W. Lin, and T.Y. Chen. 1999. Elimination of the slow gating of ClC-0 chloride channel by a point mutation. *J. Gen. Physiol.* 114:1–12.

Ludewig, U., M. Pusch, and T.J. Jentsch. 1996. Two physically distinct pores in the dimeric ClC-0 channel. *Nature.* 383:340–343.

Ludewig, U., T.J. Jentsch, and M. Pusch. 1997a. Analysis of a protein region involved in permeation and gating of the voltage-gated chloride channel ClC-0. *J. Physiol.* 498:691–702.

Ludewig, U., M. Pusch, and T.J. Jentsch. 1997b. Independent gating of single pores in CLC-0 chloride channels. *Biophys. J.* 73: 789–797.

Maduke, M., C. Miller, and J.A. Mindell. 2000. A decade of ClC chloride channels: structure, mechanism, and many unsettled questions. *Annu. Rev. Biomol. Struct.* 29:411–438.

MacKinnon, R., and C. Miller. 1988. Mechanism of charybdotoxin block of the high conductance, Ca^{2+}-activated K^+ channel. *J. Gen. Physiol.* 91:335–349.

Middleton, R.E., D.J. Pheasant, and C. Miller. 1996. Homodimeric

architecture of a ClC-type chloride ion channel. *Nature.* 383:337–340.

Miller, C. 1982. Open-state substructure of single chloride channels from *Torpedo* electroplax. *Phil. Trans. R. Soc. Lond. B.* 299:401–411.

Mindell, J.A., M. Maduke, C. Miller, and N. Grigorieff. 2001. Projection structure of a ClC-type chloride channel at 6.5 A resolution. *Nature.* 409:219–223.

Nilius, B., T. Voets, J. Eggermont, and G. Droogmans. 1999. VRAC: a multifunctional volume-regulated anion channel in vascular endothelium. *In* Chloride Channels. R. Kozlowski, editor. Isis Medical Media, Oxford, UK. 47–63.

Pusch, M., K. Steinmeyer, and T.J. Jentsch. 1994. Low single-channel conductance of the major skeletal muscle chloride channel ClC-1. *Biophys. J.* 66:149–152.

Pusch, M., U. Ludewig, A. Rehfeldt, and T.J. Jentsch. 1995. Gating of the voltage-dependent chloride channel ClC-0 by the permeant anion. *Nature.* 373:527–531.

Pusch, M., U. Ludewig, and T.J. Jentsch. 1997. Temperature dependence of fast and slow gating relaxations of ClC-0 chloride channels. *J. Gen. Physiol.* 109:105–116.

Pusch, M., A. Liantonio, L. Bertorello, A. Accardi, A. De Luca, S. Pierno, V. Tortorella, and D. Conte Camerino. 2000. Pharmacological characterization of chloride channels belonging to the ClC family by the use of chiral clofibric acid derivatives. *Mol. Pharmacol.* 58:498–507.

Rychkov, G.Y., M. Pusch, D.S. Astill, M.L. Roberts, T.J. Jentsch, and A.H. Bretag. 1996. Concentration and pH dependence of skeletal muscle chloride channel ClC-1. *J. Physiol.* 497:423-435.

Rychkov, G.Y., M. Pusch, M.L. Roberts, T.J. Jentsch, and A.H. Bretag. 1998. Permeation and block of the skeletal muscle chloride channel, ClC-1, by foreign anions. *J. Gen. Physiol.* 111:653–665.

Saviane, C., F. Conti, and M. Pusch. 1999. The muscle chloride channel CLC-1 has a double-barreled appearance that is differentially affected in dominant and recessive myotonia. *J. Gen. Physiol.* 113:457–467.

Steinmeyer, K., C. Ortland, and T.J. Jentsch. 1991. Primary structure and functional expression of a developmentally regulated skeletal muscle chloride channel. *Nature.* 354:301–304.

Terlau, H., A. Boccaccio, B.M. Olivera, and F. Conti. 1999. The block of *Shaker* K^+ channels by kappa-conotoxin PVIIA is state dependent. *J. Gen. Physiol.* 114:125–140.

Thompson, J., and T. Begenesich. 2000. Interaction between quaternary ammonium ions in the pore of potassium channels: evidence against an electrostatic repulsion mechanism. *J. Gen. Physiol.* 115:769–782.

Wollnik, B., C. Kubisch, K. Steinmeyer, and M. Pusch. 1997. Identification of functionally important regions of the muscular chloride channel ClC-1 by analysis of recessive and dominant myotonic mutations. *Hum. Mol. Genet.* 6:805–811.